

Microwave-assisted rapid synthesis of #-cyclodextrin metal-organic frameworks for size control and efficient drug loading

Botao Liu, Yaping He, Liping Han, Vikramjeet Singh, Xiaonan Xu, Tao Guo, Fanyue Meng, Xu Xu, Peter York, Zhaoxin Liu, and Jiwen Zhang

Cryst. Growth Des., **Just Accepted Manuscript** • DOI: 10.1021/acs.cgd.6b01658 • Publication Date (Web): 20 Feb 2017

Downloaded from <http://pubs.acs.org> on February 26, 2017

Just Accepted

“Just Accepted” manuscripts have been peer-reviewed and accepted for publication. They are posted online prior to technical editing, formatting for publication and author proofing. The American Chemical Society provides “Just Accepted” as a free service to the research community to expedite the dissemination of scientific material as soon as possible after acceptance. “Just Accepted” manuscripts appear in full in PDF format accompanied by an HTML abstract. “Just Accepted” manuscripts have been fully peer reviewed, but should not be considered the official version of record. They are accessible to all readers and citable by the Digital Object Identifier (DOI®). “Just Accepted” is an optional service offered to authors. Therefore, the “Just Accepted” Web site may not include all articles that will be published in the journal. After a manuscript is technically edited and formatted, it will be removed from the “Just Accepted” Web site and published as an ASAP article. Note that technical editing may introduce minor changes to the manuscript text and/or graphics which could affect content, and all legal disclaimers and ethical guidelines that apply to the journal pertain. ACS cannot be held responsible for errors or consequences arising from the use of information contained in these “Just Accepted” manuscripts.

1
2
3
4 **1 Cover Page:**

5
6 **2 Microwave-assisted rapid synthesis of γ -cyclodextrin metal-organic**
7
8
9 **3 frameworks for size control and efficient drug loading**

10
11
12
13 **4 Authors:**

14
15 Botao Liu^{1,2,a}, Yaping He^{1,3,a}, Liping Han¹, Vikramjeet Singh¹, Xiaonan Xu¹, Tao
16
17 Guo¹, Fanyue Meng¹, Xu Xu², Peter York¹, Zhaoxin Liu^{2,*}, Jiwen Zhang^{1,2,3,*}

18
19
20 **8 Affiliations:**

21
22 ¹ Center for Drug Delivery Systems, Shanghai Institute of Materia Medica, Chinese Academy of
23
24 Sciences, Shanghai 201210, China

25
26 ² School of Chemical and Environmental Engineering, Shanghai Institute of Technology, Shanghai
27
28 201418, China

29
30 ³ University of Chinese Academy of Sciences, Beijing 100049, China

31 ^{a:} Who contributed equally to the manuscript

32
33
34 **16 *Corresponding Author:**

35
36 Prof. Jiwen Zhang
37
38 Center for Drug Delivery Systems, Shanghai Institute of Materia Medica, Chinese Academy of
39
40 Sciences, No. 501 of Haike Road, Shanghai 201210, China; Tel: +86-21-20231980; E-mail:
41
42 jwzhang@simm.ac.cn.

43
44 Mr. Zhaoxin Liu
45
46 Shanghai Institute of Technology, No. 100, Haiquan Road, Shanghai 201418, China; Tel: +86-21-
47
48 60877215; E-mail: ericzliu@sina.com.

1
2
3
4 29 **Abstract**
5

6 30 The micron and nanometer sized γ -cyclodextrin metal-organic frameworks
7
8 31 (γ -CD-MOFs) were successfully synthesized using microwave technique for the first
9
10 32 time for rapid and facile synthesis. Polyethylene glycol 20000 (PEG 20000) was used
11
12 33 as surfactant to control the size and morphology of γ -CD-MOFs. The as-synthesized
13
14 34 γ -CD-MOFs were characterized using various techniques, including X-ray powder
15
16 35 diffraction (PXRD), scanning electron microscopy (SEM), thermogravimetric
17
18 36 analysis (TGA) and N₂ adsorption. The increment in the reaction time and MeOH
19
20 37 ratio dramatically damaged the crystalline integrity of γ -CD-MOFs. Fenbufen was
21
22 38 selected as a model drug to evaluate the loading characteristics of γ -CD-MOF crystals.
23
24 39 In results, the nanometer sized γ -CD-MOFs (100-300 nm) showed rapid and higher
25
26 40 adsorption (196 mg·g⁻¹) of Fenbufen in EtOH when compared with the micron
27
28 41 crystals. The adsorption parameters fitted well to a pseudo-second-order kinetic
29
30 42 model and chemisorption of Fenbufen was further supported by molecular docking
31
32 43 illustrations. In summary, the control synthesis of γ -CD-MOFs was successfully
33
34 44 achieved by microwave assisted method and resultant crystals were further evaluated
35
36 45 for potential drug delivery applications.
37
38
39
40
41
42
43
44
45

46 **Keywords:** Cyclodextrin-metal-organic frameworks; microwave; PEG 20000; drug
47 loading; crystallinity
48
49
50
51
52
53
54
55
56
57
58
59
60

49 **Title Page**50 **Microwave-assisted rapid synthesis of γ -cyclodextrin metal-organic**
51 **frameworks for size control and efficient drug loading**52
53 **Authors:**54 Botao Liu^{1,2,a}, Yaping He^{1,3,a}, Liping Han¹, Vikramjeet Singh¹, Xiaonan Xu¹, Tao
55 Guo¹, Fanyue Meng¹, Xu Xu², Peter York¹, Zhaoxin Liu^{2,*}, Jiwen Zhang^{1,2,3,*}56 **Affiliations:**57 ¹ Center for Drug Delivery Systems, Shanghai Institute of Materia Medica, Chinese Academy of
58 Sciences, Shanghai 201210, China59 ² School of Chemical and Environmental Engineering, Shanghai Institute of Technology, Shanghai
60 201418, China61 ³ University of Chinese Academy of Sciences, Beijing 100049, China62 ^{a:} Who contributed equally to the manuscript63
64 **Introduction**65 Metal-organic frameworks (MOFs) have emerged as a new class of nanoporous
66 materials with wide range of applications in molecular recognition,¹ gas storage,²
67 catalysis³ and drug delivery.⁴ Usually, they are constructed from metal ion connectors
68 and organic bridging ligands.⁵ Contrary to conventional porous material,^{6, 7} the pore
69 size and inner surface characteristics of MOFs can be modulated by tuning the size
70 and shapes of the linkers.⁸

71 The sizes and shapes of MOF materials are critical for their various applications.

72 Therefore, much efforts have been directed to shorten the synthesis time and to

1
2
3
4 73 produce uniform crystals using microwave-assisted,⁶ mechanochemical⁷ and
5
6 74 sonochemical⁸ methods. At the same time, several strategies have been adopted for
7
8
9 75 controlling the size and morphology of MOFs by altering the synthetic parameters
10
11 76 including temperature, processing duration, metal source and solvents. For example,
12
13 77 Ban et al reported the morphology control synthesis of ZIF-78 materials by adjusting
14
15 78 the nutrient and ligand concentrations.⁹ Pan et al reported a facile synthesis method
16
17 79 using cetyl trimethyl ammonium bromide as a capping agent for controlling the size
18
19
20
21 80 and morphology of ZIF-8 crystals in aqueous systems.¹⁰ Cheng et al presented a
22
23 81 solvothermal method for control synthesis of NH₂-MIL-53 by altering the DMF and
24
25
26 82 water ratio without adding any surfactants or capping agents.¹¹

27
28
29 83 In recent years, there has been a growing interest in encapsulating drugs in MOFs
30
31 84 (Table S1). However, it is very necessary to consider the biocompatibility of material
32
33 85 compositions for biomedical applications. Thus, appropriate natural molecules such as
34
35 86 amino acid,¹² peptides¹³ and nucleobases¹⁴ as well as metal ions (Ca, Mg, Zn, Fe) are
36
37
38 87 considered to be biocompatible as organic linkers and metal connectors of MOFs,
39
40
41 88 respectively. In addition, some post-synthetic modifications of MOFs with biofriendly
42
43
44 89 functionalized linkers also showed their advantages over other reactive groups in
45
46 90 various structures.^{15,16}

47
48
49 91 Recently, Stoddart et al reported the synthesis of environmental friendly and
50
51 92 renewable cyclodextrin metal-organic frameworks (CD-MOFs) through a
52
53 93 vapor-diffusion method.¹⁷ The CD-MOFs are body-centered cubic extended structures
54
55
56 94 prepared from the coordination of γ -CD and potassium ion and possessed large
57
58
59
60

1
2
3
4 95 spherical voids of 17 Å with apertures of 7.8 Å. Among the various MOFs reported so
5
6 96 far, CD-MOFs are materials with potential to adsorb gases (N₂, H₂, CO₂ and CH₄) and
7
8 97 some other molecules (Rhodamine B and 4-Phenylazophenol) within their pores.¹⁷
9
10 98 Taking advantage of their uniform channels (17 Å) and high local concentrations of
11
12 99 OH⁻ ions, the γ-CD-MOFs were used as template for the synthesis of silver and gold
13
14 100 nanoparticles.¹⁸
15
16 101 The original vapor diffusion method was able to produce cubic crystals (40-500 μm)
17
18 102 of γ-CD-MOFs at ambient temperature over the period of a week.¹⁷ A modified
19
20 103 method with the addition of CTAB and a controlled incubation time of 26-32 h has
21
22 104 been reported to produce γ-CD-MOF crystals, and they succeeded in the preparation
23
24 105 of good quality crystals with well-defined shape in the range of several hundred
25
26 106 nanometers to millimeters.¹⁹ However, vapor diffusion method is very difficult to
27
28 107 fabricate MOFs for mass production and future industrial use. Not long before, a
29
30 108 further improved approach for size control of γ-CD-MOFs has also been reported by
31
32 109 us with a conventional vapor diffusion technique, which took about 6 hours.²⁰ In
33
34 110 addition, the previous size modulator of CTAB was quite toxic for cells.
35
36 111 In this paper, we report a fast synthesis of γ-CD-MOFs within several minutes under
37
38 112 microwave irradiation. More importantly, PEG 20000, a pharmaceutical excipient,
39
40 113 was used as the size modulator for the first time herein. In addition, we could
41
42 114 efficiently control the size and morphology of the obtained γ-CD-MOF crystals well
43
44 115 by optimizing the reaction time, temperature and solvent ratio in the synthesis process.
45
46 116 Fenbufen was selected as drug candidate to investigate the drug loading behavior of
47
48
49
50
51
52
53
54
55
56
57
58
59
60

1
2
3
4 117 the crystals.

5
6 118 **Experimental Section**

7
8
9 119 **Materials and Physical Measurements**

10
11 120 γ -cyclodextrin (γ -CD, MaxDragon biochem Ltd), potassium hydroxide (KOH, 85.0%,
12
13 Sinopharm Chemical Reagent Co., Ltd), methanol (MeOH, 99.5%, Sinopharm
14
15 Chemical Reagent Co., Ltd), polyethylene glycol 20000 (PEG 20000, MW ~ 20000,
16
17 Ourchem, Sinopharm Chemical Reagent Co., Ltd), ethanol (EtOH, 99.7%, Sinopharm
18
19 Chemical Reagent Co., Ltd) and dichloromethane (DCM, 99.5%, Sinopharm
20
21 Chemical Reagent Co., Ltd). Fenbufen (FBF, >99.5% purity) was purchased from
22
23 Dalian Meilun Biotech Co., Ltd (China). Pure water (18.4 M Ω cm) used in all
24
25 experiments was purified by a Milli-Q system (Millipore, Milford, MA, USA). All
26
27 other chemicals were of analytical grade and used without further purification.
28
29
30
31
32

33
34 129 **Synthesis of γ -CD-MOFs**

35
36 130 A mother solution (Figure S1) was prepared by mixing γ -CD (324 mg) and KOH (112
37
38 mg) in pure water (10 mL) with pre-addition of 6 mL MeOH, which was sealed and
39
40 placed in a glass vessel. The mixed solution was heated at 40 ~ 100 °C through
41
42 microwave irradiation (CEM, Discover, USA) with power (100 w) for 1 ~ 120 min
43
44 and the clear solution was obtained. Then 256 mg of PEG 20000 was added quickly to
45
46 trigger the rapid deposition of crystalline materials (precipitation). 60 min later, the
47
48 micron sized MOF crystals were collected after separation, washed with 15 mL EtOH
49
50 and MeOH twice and dried overnight at 50°C under vacuum. In parallel experiments,
51
52 the size of the γ -CD-MOF crystals was modulated by altering the different processing
53
54
55
56
57
58
59
60

1
2
3
4 139 parameters such as, reaction time (t), temperature (T), solvent ratio (R) of water to
5
6 140 MeOH (v/v) and modulators (M). The synthesis procedure of nanometer sized crystals
7
8
9 141 was the same as that for micron sized γ -CD-MOFs. During the size modulation
10
11 142 process, 16 mL of MeOH with/without 128 mg of PEG 20000 was added to the
12
13 143 reaction solution (F14 and F15) and the final solution was then heated at 50 °C for 10
14
15 144 min. The resulting samples were identified as F1 to F15, the conditions employed in
16
17 145 the controlled preparation and the morphology results of these samples are
18
19 146 summarized in Table 1. In comparison, the preparation of γ -CD-MOFs (identified as
20
21 147 F16) by conventional vapor diffusion method was also investigated according to
22
23 148 Smaldone's work (Supporting information S1).¹⁷
24
25
26
27
28
29
30
31
32

33 **Table 1.** Summary of synthesis conditions of F1-F15 samples

Samples	Heating time, t (min)	T (°C)	R	M	Incubation time, t (min)	Results (Morphology)
F1	1	50	10: 6	PEG 20000	60	Typical cubes
F2	10	50	10: 6	PEG 20000	60	Typical cubes
F3	20	50	10: 6	PEG 20000	60	Typical cubes
F4	60	50	10: 6	PEG 20000	60	Typical cubes
F5	120	50	10: 6	PEG 20000	60	Typical cubes
F6	10	40	10: 6	PEG 20000	60	Non-typical Cubes
F7	10	60	10: 6	PEG 20000	60	Typical cubes
F8	10	80	10: 6	PEG 20000	60	Typical cubes
F9	10	100	10: 6	PEG 20000	60	Typical cubes
F10	10	50	10: 4	PEG 20000	60	Non-typical hexagonal shapes
F11	10	50	10: 5	PEG 20000	60	Non-typical Cubes
F12	10	50	10: 7	PEG 20000	60	Typical cubes
F13	10	50	10: 8	PEG 20000	60	Typical cubes
F14	10	50	10: 6	MeOH	60	Non-typical Cubes
F15	10	50	10: 6	MeOH + PEG 20000	60	Non-typical Cubes

34
35
36
37
38
39
40
41
42
43
44
45
46
47
48
49
50
51
52
53
54
55
56
57
58
59
60

152 **Characterizations of γ -CD-MOFs**

153 Morphological characterizations of γ -CD-MOF crystals were conducted by the
154 scanning electron microscope (SEM, S3400, Hitachi). The specimens were
155 immobilized on a metal stub with double-sided adhesive tape and coated with a thin
156 gold film, and then observed under definite magnification.

157 The crystallinity of the samples was characterized by X-ray powder diffraction
158 (PXRD) analysis. Diffraction patterns of the prepared γ -CD-MOF crystals were
159 detected with a Bruker D8 Advance diffractometer (Bruker, Germany) at ambient
160 temperature, with tube voltage of 40 kV, tube current of 40 mA in a stepwise scan
161 mode ($8^\circ \cdot \text{min}^{-1}$). All the samples were irradiated with monochromatized $\text{CuK}\alpha$
162 radiation and analyzed over a 2θ angle range of $3 - 40^\circ$.

163 Thermogravimetric analysis (TGA) of γ -CD-MOF crystals was performed using a
164 thermal analysis system (NETZSCH 209F3 240-20-382-L, USA) at a heating rate of
165 $10^\circ \text{C} \cdot \text{min}^{-1}$ under nitrogen. Samples were weighed (approx. 5 mg) in a hanging
166 aluminum pan and the weight loss percentage of the samples was monitored from 30
167 to 400°C .

168 Nitrogen adsorption-desorption isotherm was measured with a liquid nitrogen bath
169 (-196°C) using a porosimeter (Micromeritics ASAP 2020, USA). In order to remove
170 the interstitial solvents, the samples were activated by immersing in dichloromethane
171 for three days and dried under vacuum at 50°C for 12 h. Known amounts of samples
172 (e. g. 150-200 mg) were loaded into the BET (Langmuir) sample tubes and degassed
173 under vacuum (10^{-5} Torr) at 50°C for 6 h. BET (Langmuir) model was applied to

1
2
3
4 174 measure the specific surface areas of the prepared samples.

5
6 175 FT-IR spectra of samples were obtained using an FT-IR spectrometer (Nicolet
7
8
9 176 Continuum XL, Thermo Fisher Scientific). Briefly, the sample and potassium bromide
10
11 177 were mixed well with a ratio of 1:10 followed by being compressed into a disk. 32
12
13 178 scans were carried out in wavenumber 400-4000 cm^{-1} at a resolution of 4 cm^{-1} .

16 179 **Adsorption experiment**

17
18
19 180 In order to investigate the adsorption behavior of γ -CD-MOFs for FBF in EtOH
20
21 181 solution, 50 mg of γ -CD-MOFs were added into 25 mL of FBF solution (600
22
23 182 $\mu\text{g} \cdot \text{mL}^{-1}$) at 30 $^{\circ}\text{C}$ temperature. The suspensions were shaken (150 rpm) and
24
25 183 incubated for 24 h. The FBF content of the solution was determined followed by a
26
27 184 HPLC method. The adsorption capacity (q) of γ -CD-MOFs towards FBF was
28
29 185 calculated as follows:

$$32 \quad 33 \quad 34 \quad 186 \quad q_t = \frac{V(C_0 - C_t)}{W} \quad (1)$$

35
36 187 where q_t ($\mu\text{g} \cdot \text{mg}^{-1}$) is the adsorption capacity at contact time t , V is the volume of
37
38 188 FBF solution (mL), C_0 is the initial concentration of FBF ($\mu\text{g} \cdot \text{mL}^{-1}$), C_t is the
39
40 189 concentration of FBF at contact time t ($\mu\text{g} \cdot \text{mL}^{-1}$), and W is the weight of CD-MOFs
41
42 190 (mg).

43
44
45 191 Release of FBF from FBF loaded CD-MOFs in EtOH was also performed. And the
46
47 192 detailed methods and results were described in Supporting Information (S5 and Figure
48
49 193 S7).

51 194 **HPLC method for determination of FBF**

52
53
54 195 The analysis was carried out with an Agilent C18 column (4.6 mm \times 150 mm, 3.6 μm
55
56 196 i.d.) using flow rate of 1.0 $\text{mL} \cdot \text{min}^{-1}$ at a wavelength of 281 nm. The FBF was

1
2
3 197 detected with the column temperature of 25 °C, the injection volume of 2 µL and the
4
5 198 mobile phase composed of 10% acetonitrile in 0.1% formic acid aqueous solution,
6
7 199 changing linearly over 10 min to 90% acetonitrile maintained for 3 min, and then
8
9 200 decreasing to 10% in 1 min maintained for 6 min.

201 **Molecular docking of FBF and γ -CD-MOFs**

202 The crystal structure of CD-MOFs was extracted from single crystal structure of
203 CD-MOFs in literature.²¹ In the docking model, an expanded non-periodic structure
204 was used, in which the K⁺ ion that not affecting rigid docking results was deleted and
205 the OH⁻ ion was replaced by H₂O. The structure of sucralose molecule was built using
206 the Materials Visualizer module in Materials Studio (MS, Accelrys Inc.) 5.0. The
207 Forcite module in MS was employed for minimization and molecular dynamics (MD)
208 simulation. The docking program AutoDock Vina 1.1.2 was used to perform the
209 automated molecular docking calculation.²² Detailed method was described in S4.

210 **Results and discussion**

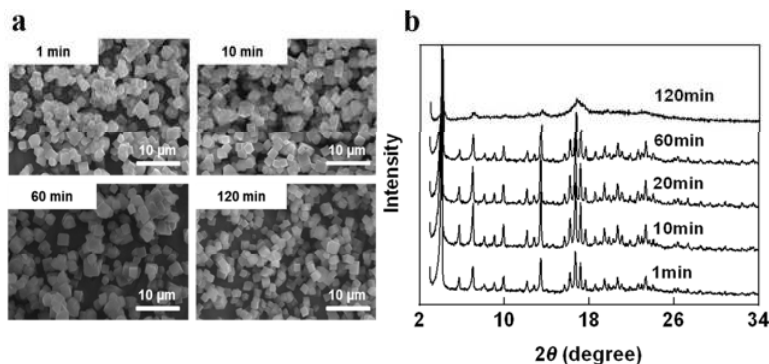
211 In this study, γ -CD-MOFs were synthesized by a microwave irradiation method of
212 γ -CD and KOH in a 1: 8 molar ratio under different reaction conditions. Cubic
213 γ -CD-MOF crystals were obtained by raising the reaction temperature and
214 pre-addition of sufficient reaction solvent. To the best of our knowledge, this is the
215 first report on synthesis of γ -CD-MOFs using microwave irradiation method and PEG
216 as an efficient size modulator. The synthesis procedure was thoroughly optimized as
217 explained in following sections.

218 **Effects of reaction parameters on crystal assembling**

219 Initial investigations revealed that reaction time and solvent ratio were critical to the
220 fabrication of γ -CD-MOFs crystals in microwave irradiation method. Different time

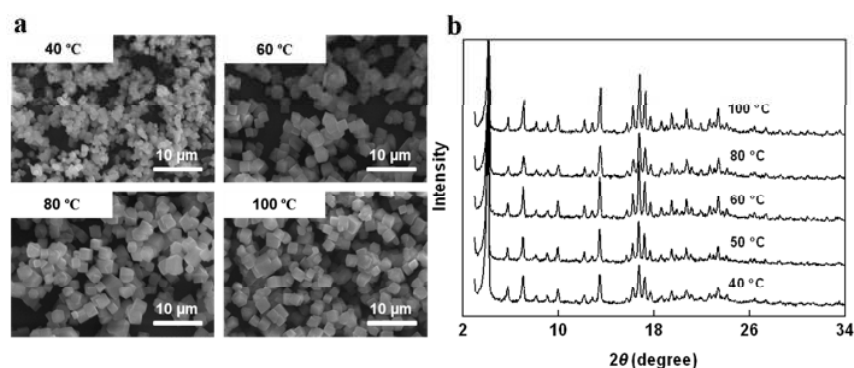
1
2
3
4 221 parameters from 1 min to 120 min were considered for the optimization of reaction
5
6 222 time. The SEM images of the crystals synthesized at different time intervals revealed
7
8 223 the uniform cubic morphologies as shown in Figure 1a. The size of γ -CD-MOFs
9
10 224 crystals (1-3 μm) just modulated by PEG 20000 were recorded smaller when
11
12 225 compared with those obtained with CTAB by vapor diffusion method,¹⁹ which might
13
14 226 be due to the higher number of nucleation sites.
15
16
17

18
19 227 The PXRD results in Figure 1b suggested the high crystallinity of the samples
20
21 228 synthesized at different time intervals in agreement with the crystals synthesized by
22
23 229 conventional method (Figure S2) and the reported literature.¹⁹ However, the dramatic
24
25 230 loss in crystallinity was recorded for prolonged reaction time of 120 min in spite of
26
27 231 their cubic shapes. The microwave thermal effects are characterized as a local heating
28
29 232 state. While the heating time is increased beyond the optimum level, such
30
31 233 deterioration in cubic structure of CD-MOFs may be observed to some extent. Similar
32
33 234 phenomenon was also found in the synthetic process of some other samples.²³
34
35
36
37
38
39
40
41



53
54 **Figure 1.** SEM morphology images and PXRD crystallinity patterns of γ -CD-MOF crystals
55
56 238 obtained after different time of 1 (F1), 10 (F2), 60 (F4) and 120 (F5) min. The longer reaction time
57
58 239 of 120 min showed the destruction of the crystalline structure of γ -CD-MOFs.
59
60

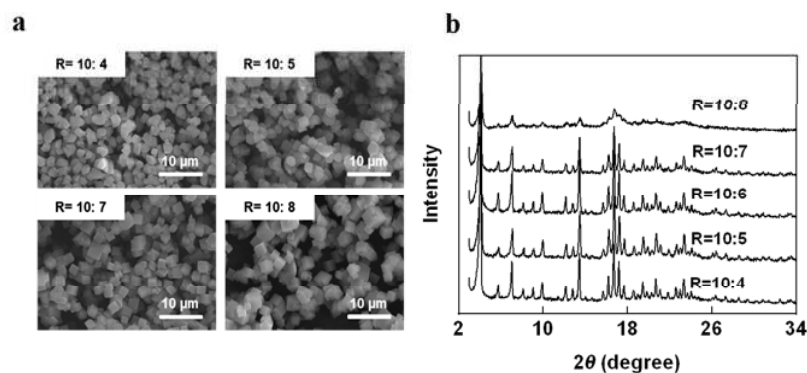
1
2
3 241 In addition to the reaction time, the effect of temperature on the size and morphology
4
5 242 of γ -CD-MOFs was also investigated. SEM images of γ -CD-MOF crystals obtained at
6
7 243 different reaction temperature of 40, 60, 80 and 100 °C at 10 min were shown in
8
9 244 Figure 2a. A significant effect of reaction temperature on the size of γ -CD-MOF
10
11 245 crystals was recorded. At lower temperatures, the deposition of white precipitates
12
13 246 were observed with the pre-addition of MeOH into the γ -CD/KOH mother solution.
14
15 247 The precipitates did not dissolve completely at 40 °C and this observation can be
16
17 248 attributed to the rapid over-saturation of the precursors due to pre-addition of
18
19 249 excessive MeOH. During the crystallization process, the anti-solvent recrystallization
20
21 250 process would be easier and the size of the newly obtained crystals would be
22
23 251 functioned by the recrystallization and the size modulator of PEG 20000, finally led to
24
25 252 the formation of smaller size of γ -CD-MOF crystals. In order to better control crystals
26
27 253 size, the increase of the temperature must be processed. With an further increase of
28
29 254 temperature from 50 °C to 100 °C, no distinct influence on the size and morphology
30
31 255 of γ -CD-MOFs crystals was observed. The crystalline structure (Figure 2 b) of
32
33 256 γ -CD-MOFs does not change with the reaction temperature.



38
39
40
41
42
43
44
45
46
47
48
49
50 257
51 258 **Figure 2.** SEM morphology images and PXRD crystallinity patterns of γ -CD-MOF crystals
52 259 obtained at different temperature of 40 (F6), 60 (F7), 80 (F8) and 100 °C (F9). The increase of
53 260 temperature from 40 to 100 °C showed no influence on the crystalline structure of γ -CD-MOFs.
54 261

55
56 262 γ -CD-MOF crystals with different morphologies were obtained by varying the solvent
57
58
59
60

1
2
3 263 ratio (MeOH in MeOH-H₂O) at 10 min and 50 °C. Figure 3a showed the SEM images
4
5 264 of the samples synthesized with different water to MeOH ratios. Initially with low
6
7 265 MeOH volume, the irregular hexagonal crystals were produced. With increasing the
8
9
10 266 proportion of MeOH to 37.5 vol% at same water content, the uniform cubic crystals
11
12 267 were obtained. It was speculated that increment in MeOH volume contributes to the
13
14 268 nucleation of MOF crystals due to the thermodynamic stability of crystal face growth.
15
16 269 Crystal shape is often a consequence of the coexistence of slower and faster growth
17
18 270 facets. With the growth of the crystal, the crystal morphology is dominated by the
19
20
21 271 slower growth facets.²⁴ Crystalline patterns of γ -CD-MOFs synthesized with different
22
23 272 solvent ratios were presented in Figure 3b. It is well-known that the low
24
25 273 supersaturation often leads to a decrease in nucleation sites.²⁵ We expected that less
26
27 274 volume of MeOH does not satisfy the level of supersaturation sufficient for the
28
29
30 275 crystals growth. However, it was also observed that excessive volume of MeOH
31
32 276 (water: MeOH = 10: 8) would also deteriorate the crystallinity of γ -CD-MOFs.



277

278 **Figure 3.** SEM morphology images and PXRD crystallinity patterns of γ -CD-MOF crystals
279 obtained with different ratios of H₂O to MeOH as 10: 4 (F10), 10: 5 (F11), 10: 7 (F12) and 10: 8
280 (F13). Higher volume ratios of MeOH resulted in γ -CD-MOFs more uniform but caused
281 disturbance of the crystallinity of γ -CD-MOFs.

282

283 **Size modulator effects**

284

285

286

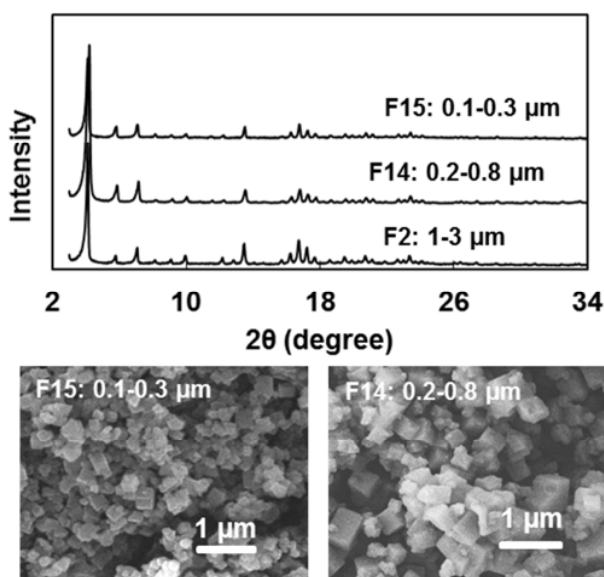
287

288

289

290

1
2
3 284 The smaller crystal size in nanometer range could be promising for biological
4
5 285 applications and traditional selective separation and catalysis. The crystal size can be
6
7 286 adjusted by controlling the nucleation and crystal growth rate.²⁶ Micron sized
8
9
10 287 γ -CD-MOF crystals can be obtained by simply adding the PEG 20000 as surfactant.
11
12 288 MeOH was employed as a size modulator to obtain the nanometer sized crystals.
13
14 289 Crystal size of 200-800 nm was recorded by SEM as shown in Figure 4. Furthermore,
15
16 290 much smaller crystals of 100-300 nm were obtained by pre-mixing of MeOH with
17
18 291 PEG 20000 during modulation process. The crystallinity of nano crystals were found
19
20 292 consistent with those of micron sized crystals as shown in Figure 4. Smaller crystals
21
22 293 are usually obtained when the nucleation rate is larger than the rate of crystal
23
24 294 growth.²⁷ It could be easily understood that excess volume of MeOH contributed to
25
26 295 the oversaturation of the reaction solution, finally resulted in a dramatic decrease of
27
28
29
30 296 CD-MOF size.



297

54
55 298 **Figure 4.** PXRD crystallinity patterns and SEM morphology images of γ -CD-MOF crystals. It
56 299 shows different sizes of γ -CD-MOFs possess the similar PXRD pattern.

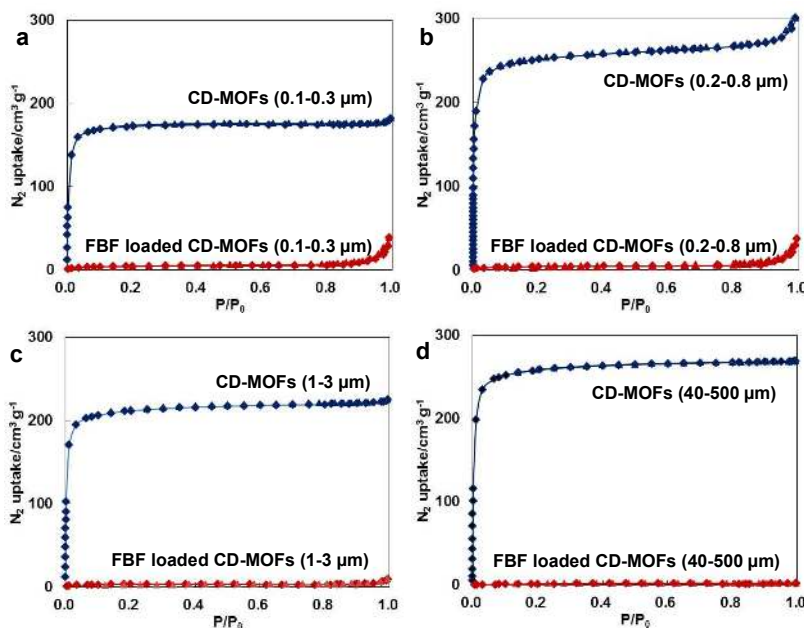
57
58 300

1
2
3
4 301 **Adsorption isotherms of FBF on γ -CD-MOFs**

5
6 302 TGA data (Figure S 4) for DCM treated samples revealed a thermal stability region of
7
8
9 303 crystals following the initial loss due to residual solvent guest molecules. These
10
11 304 results directed us to evaluate the porosity of CD-MOF crystals. Not long before, a
12
13 305 total of 21 types of model drugs were screened to testify the adsorption capacity of
14
15 306 γ -CD-MOFs, wherein, γ -CD-MOFs showed the highest captopril adsorption
16
17 307 capability which reached to 19.3% (w/w).²⁰ Later, sucralose, a kind of non-nutritive
18
19 308 sweetener was loaded by γ -CD-MOFs and the thermal stability of this drug was
20
21 309 successfully improved, in which the drug loading efficiency for CD-MOF-Micro and
22
23 310 CD-MOF-Nano was 17.5 ± 0.9 % and 27.9 ± 1.4 % (w/w), respectively.²⁸

24
25
26 311 The N₂ adsorption-desorption isotherms (Figure 5) of activated γ -CD-MOFs of F15
27
28 312 (0.1-0.3 μ m), F14 (0.2-0.8 μ m), F2 (1-3 μ m) and F16 (40-500 μ m) (Figure S3)
29
30 313 defined a BET (Langmuir) surface area of 673 (751), 1010 (1175), 820 (913) and
31
32 314 1002 (1118) m²·g⁻¹, respectively. The above BET surface area results clearly
33
34 315 illustrated that the surface area of samples of F14 and F16 were larger than others,
35
36 316 which obviously indicated that the size modulator of PEG 20000 diminished the BET
37
38 317 surface area of γ -CD-MOF crystals. The sample of F15 possessed the lowest BET
39
40 318 surface area among these four samples, which could also be due to that some cavities
41
42 319 of CD-MOFs being blocked by PEG 20000 molecules. However, the drug adsorption
43
44 320 properties of γ -CD-MOFs crystals could not be directly estimated from BET results.
45
46 321 Thus, systematic adsorption experiments were set up to optimize their drug adsorption
47
48 322 abilities.
49
50
51
52
53
54
55
56
57
58
59
60

323 Fenbufen, an analgesic and non-steroidal anti-inflammatory drug with a low aqueous
 324 solubility and weak acidic nature, was selected for adsorption evaluations. The
 325 dimensions of aperture window (7.8 Å) and internal pores (17 Å) are sufficiently large
 326 to accommodate the FBF because of its small molecular size. In view of MOFs with
 327 different sizes showing different adsorption capabilities towards same small molecular
 328 sized compounds²⁹, the adsorption capability to FBF was investigated using micron
 329 and nanometer sized γ -CD-MOFs. The specific sizes and BET (Langmuir) surface
 330 area results of used γ -CD-MOFs crystals are detailed in Table 2.



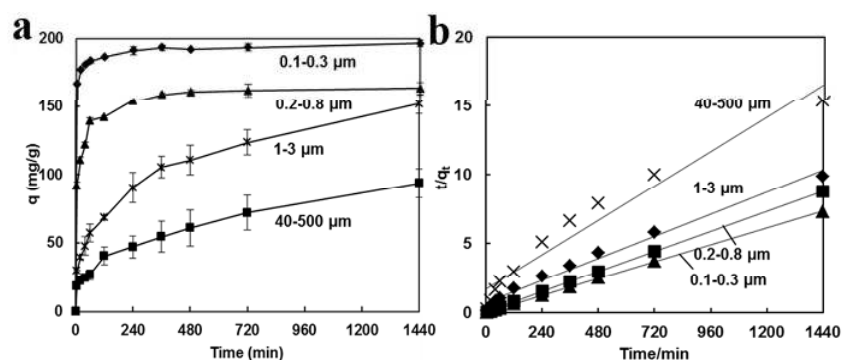
331
 332 Figure 5. N₂ Adsorption isotherms, for activated and FBF-loaded samples of γ -CD-MOFs of (a)
 333 F15 (0.1-0.3 μm), (b) F14 (0.2-0.8 μm), (c) F2 (1-3 μm) and (d) F16 (40-500 μm) measured at 77
 334 K. The N₂ uptake defines a BET (Langmuir) surface area of 673 (751) (F15), 1010 (1175) (F14),
 335 820 (913) (F2) and 1002 (1118) (F16) $\text{m}^2 \cdot \text{g}^{-1}$.

336
 337 The effect of FBF incubation time on adsorption capacity is shown in Figure 6a.
 338 Gradual increment in adsorption content was noticed with the prolongation of time
 339 but varied in micron and nanometer sized γ -CD-MOFs. The crystals of 100-300 nm

1
 2
 3
 4 340 (F15) exhibited a rapid and higher adsorption capacity for FBF compared with other
 5
 6 341 γ -CD-MOFs. The F15 sample showed a rapid adsorption during the first 1 h and
 7
 8
 9 342 reached the adsorption equilibrium within 2 h with the highest adsorption capacity of
 10
 11 343 196 mg·g⁻¹ (molar ratio of FBF to CD-MOFs was 1: 1.9). Obviously, the adsorption
 12
 13
 14 344 content of sample F15 in 5 min was similar to that of sample F16 within 24 h.
 15
 16 345 The obtained data was fitted well to pseudo-second-order kinetic model (see S3 for
 17
 18
 19 346 method details) which suggested the chemisorption behavior of drug adsorption.^{30,31}
 20
 21 347 The coefficients for the linear plots of t/q_t against time for pseudo-second-order
 22
 23
 24 348 kinetics were greater than 0.99 for all systems except F16 ($r^2 = 0.95$, Figure 6b) which
 25
 26 349 might be due to the non-uniformity of F16 crystal sizes. The proposed hypothesis that
 27
 28
 29 350 the FBF molecules occupied most of the crystals cavities was supported by a dramatic
 30
 31 351 decrease in the surface areas of the F2, F14, F15 and F16 crystals (Table 2 and Figure
 32
 33
 34 352 5). Furthermore, the release rates of FBF loaded γ -CD-MOFs in EtOH were very
 35
 36 353 similar with the adsorption process and the cumulative release percentages of the four
 37
 38
 39 354 samples within 20 h kept 70-85 % (Figure S7).
 40
 41
 42
 43
 44
 45
 46
 47
 48
 49
 50
 51
 52
 53
 54
 55
 56
 57
 58
 59
 60

356 **Table 2.** Summary of the size of γ -CD-MOFs (F2, F14, F15, F16)

Samples	Size (μm)	BET (Langmuir) surface area ($\text{m}^2 \cdot \text{g}^{-1}$)
F2	1-3	820 (913)
F14	0.2-0.8	1010 (1175)
F15	0.1-0.3	673 (751)
F16	40-500	1002 (1118)



357
358 **Figure 6.** (a) Effects of contacted time on the adsorption of FBF onto Micro and Nanometer sized
359 γ -CD-MOFs ($n=2$) of F15 (0.1-0.3 μm), F14 (0.2-0.8 μm), F2 (1-3 μm) and F16 (40-500 μm). The
360 crystals with smaller size distinctly show a higher adsorption capacity than larger size CD-MOF
361 crystals. (b) The fitting results of the pseudo-second-order kinetics fit the experimental data well.

362

363

364 FT-IR spectra and molecular docking of FBF and γ -CD-MOFs

365 The FT-IR spectra of FBF loaded γ -CD-MOFs (F2) samples are shown in Figure 7 in

366 comparison with γ -CD-MOFs and pure FBF. The characteristic C=O stretching

367 vibrations at 1712 cm^{-1} (carboxylic acid) and 1679 cm^{-1} (ketone), the skeletal

368 vibration of phenyl rings at 1600 cm^{-1} , asymmetric and symmetric vibration of

369 carboxylate groups at 1561 and 1402 cm^{-1} were observed for pure FBF. The C=O

370 stretching vibrations at 1712 cm^{-1} disappear/shift after adsorption, providing an

371 indication that FBF molecules are loaded in the cavities of γ -CD-MOFs rather than

372 adsorbed on the surface of the composites.

373 In order to explain the mechanism of FBF loading by γ -CD-MOFs, computer based

374 molecular docking studies of FBF and γ -CD-MOFs were undertaken. In the case of

375 1:2 molar ratio for γ -CD and FBF in γ -CD-MOFs, the docking free energy was

376 recorded -7.0 $\text{kcal}\cdot\text{mol}^{-1}$ and -8.5 $\text{kcal}\cdot\text{mol}^{-1}$ (Figure S5) for the first and second

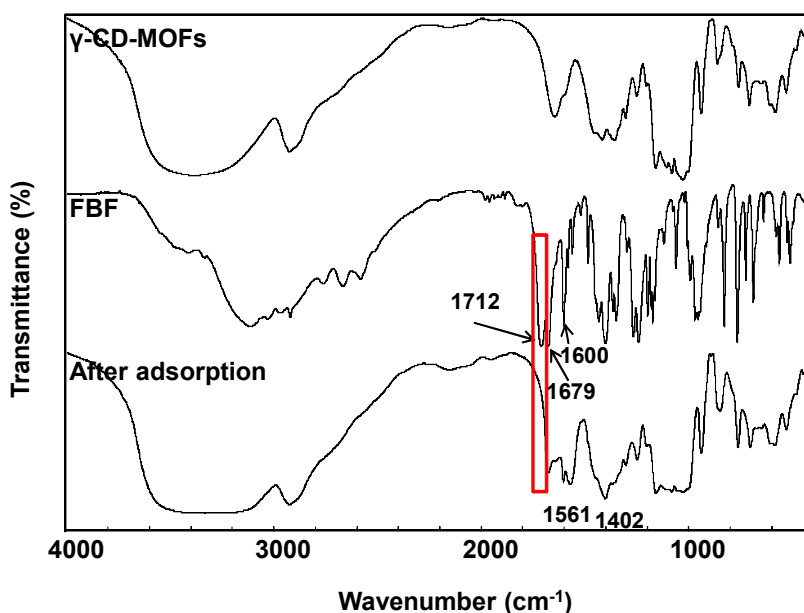
377 molecules of FBF, respectively. The simulation results suggested that the two FBF

378 molecules would be favorably positioned in the cavities of D- γ -CDs (dual γ -CD units)

379 of γ -CD-MOFs and the cavity of each γ -CD included one FBF molecule (detailed

380 docking results are described in S4). Figure S6 illustrated that H-bonds can be readily

1
2
3 381 formed by the carbonyl (-COOH) of FBF with the hydroxyl of D- γ -CDs in
4
5 382 γ -CD-MOFs, supported by the shift of C=O stretching vibrations at 1712 cm⁻¹ to
6
7 383 lower wave number in IR spectra. Considering the carboxyl function group and a
8
9
10 384 small pK_a, the high adsorption capability of γ -CD-MOFs for FBF is believed to arise
11
12 385 from the strong electrostatic interaction between the carbonyl group in FBF molecule
13
14 386 and potassium ions in γ -CD-MOFs.



387
388 **Figure 7.** FT-IR spectra of γ -CD-MOFs, FBF and FBF loaded γ -CD-MOFs, respectively.
389

390 Conclusions

391 Microwave method for rapid and controlled synthesis of γ -CD-MOFs was reported.
392 The developed method was able to shorten the hours' long fabrication process into
393 minutes. The size and morphology of γ -CD-MOF crystals have been adjusted by
394 altering the reaction time, temperature and solvent ratio. The PEG 20000 and/or
395 MeOH were successfully employed as size modulators to obtain the nanometer sized
396 crystals. Notably, an increase in the reaction time or MeOH ratio was found to

1
2
3
4 397 damage the γ -CD-MOF crystallinity. The nanometer sized γ -CD-MOFs exhibited a
5
6 398 faster and higher adsorption capability of 196 mg·g⁻¹ for FBF within 24 h compared
7
8
9 399 with the micron sized. Adsorption kinetics of FBF towards γ -CD-MOFs (600 μ g·
10
11 400 mL⁻¹ in EtOH) is described by the pseudo-second-order kinetic model. Molecular
12
13
14 401 docking further illustrated that FBF is likely to be chemisorbed by γ -CD-MOFs. Thus,
15
16 402 facile synthesis and size control approaches, together with FBF loading behavior of
17
18
19 403 γ -CD-MOF crystals are providing support for their potential applications in drug
20
21 404 delivery.

22 23 405 **Acknowledgements**

24
25
26 406 We are grateful for the financial support from Natural Science Foundation of
27
28 407 China (81373358, 81430087) and National Science and Technology Major Project
29
30 408 (2013ZX09402103).

31 32 409 **Supporting Information**

33
34
35 410 Figure S1 to S7 showing synthesis scheme, SEM, PXRD, molecular
36
37 411 docking results and FBF release.

38 39 40 412 41 42 413 **References**

- 43
44
45 414 (1) Liao, W. M.; Shi, H. T.; Shi, X. H.; Yin, Y. G., Pyrolytic cavitation, selective adsorption and molecular
46 415 recognition of a porous Eu(III) MOF. *Dalton Transactions* **2014**, 43, (41), 15305-15307.
47
48 416 (2) Luebke, R.; Weseliński, Ł. J.; Belmabkhout, Y.; Chen, Z.; Wojtas, Ł.; Eddaoudi, M., Microporous
49 417 Heptazine Functionalized (3,24)-Connected rht-Metal–Organic Framework: Synthesis, Structure, and
50 418 Gas Sorption Analysis. *Crystal Growth & Design* **2014**, 14, (2), 414-418.
51
52 419 (3) Nguyen, H. G. T.; Weston, M. H.; Sarjeant, A. A.; Gardner, D. M.; An, Z.; Carmieli, R.; Wasielewski,
53 420 M. R.; Farha, O. K.; Hupp, J. T.; Nguyen, S. T., Design, Synthesis, Characterization, and Catalytic
54 421 Properties of a Large-Pore Metal–Organic Framework Possessing Single-Site Vanadyl(monocatecholate)
55 422 Moieties. *Crystal Growth & Design* **2013**, 13, (8), 3528-3534.
56
57 423 (4) Li, Q. L.; Wang, J. P.; Liu, W. C.; Zhuang, X. Y.; Liu, J. Q.; Fan, G. L.; Li, B. H.; Lin, W. N.; Man, J. H., A
58 424 new (4,8)-connected topological MOF as potential drug delivery. *Inorg. Chem. Commun.* **2015**, 55,

- 1
2
3 425 8-10.
4 426 (5) Zou, G.-D.; He, Z.-Z.; Tian, C.-B.; Zhou, L.-J.; Feng, M.-L.; Zhang, X.-D.; Huang, X.-Y., Microwave and
5 427 Conventional Hydro(solvo)thermal Syntheses of Three Co(II) Coordination Polymers: Supramolecular
6 428 Isomerism and Structural Transformations Accompanied by Tunable Magnetic Properties. *Crystal*
7 429 *Growth & Design* **2014**, 14, (9), 4430-4438.
8 430 (6) Khan, N. A.; Jhung, S. H., Synthesis of metal-organic frameworks (MOFs) with microwave or
9 431 ultrasound: Rapid reaction, phase-selectivity, and size reduction. *Coord. Chem. Rev.* **2015**, 285, 11-23.
10 432 (7) Pilloni, M.; Padella, F.; Ennas, G.; Lai, S.; Bellusci, M.; Rombi, E.; Sini, F.; Pentimalli, M.; Delitala, C.;
11 433 Scano, A., Liquid-assisted mechanochemical synthesis of an iron carboxylate Metal Organic Framework
12 434 and its evaluation in diesel fuel desulfurization. *Microporous & Mesoporous Materials* **2015**, 213,
13 435 14-21.
14 436 (8) Bigdeli, M.; Morsali, A., Sonochemical synthesis of a nano-structured zinc(II) amidic pillar metal-
15 437 organic framework. *Ultrason. Sonochem.* **2015**, 27, 416-422.
16 438 (9) Ban, Y.; Li, Y.; Liu, X.; Peng, Y.; Yang, W., Solvothermal synthesis of mixed-ligand metal-organic
17 439 framework ZIF-78 with controllable size and morphology. *Microporous Mesoporous Mater.* **2013**, 173,
18 440 29-36.
19 441 (10) Pan, Y.; Heryadi, D.; Zhou, F.; Zhao, L.; Lestari, G.; Su, H.; Lai, Z., Tuning the crystal morphology
20 442 and size of zeolitic imidazolate framework-8 in aqueous solution by surfactants. *CrystEngComm* **2011**,
21 443 13, (23), 6937.
22 444 (11) Cheng, X.; Zhang, A.; Hou, K.; Liu, M.; Wang, Y.; Song, C.; Zhang, G.; Guo, X., Size- and
23 445 morphology-controlled NH₂-MIL-53(Al) prepared in DMF-water mixed solvents. *Dalton Trans* **2013**, 42,
24 446 (37), 13698-705.
25 447 (12) Hou, J.-J.; Xu, X.; Jiang, N.; Wu, Y.-Q.; Zhang, X.-M., Selective adsorption in two porous triazolate-
26 448 oxalate-bridged antiferromagnetic metal-azolate frameworks obtained via in situ decarboxylation of
27 449 3-amino-1,2,4-triazole-5-carboxylic acid. *J. Solid State Chem.* **2015**, 223, 73-78.
28 450 (13) Katsoulidis, A. P.; Park, K. S.; Antypov, D.; Marti-Gastaldo, C.; Miller, G. J.; Warren, J. E.; Robertson,
29 451 C. M.; Blanc, F.; Darling, G. R.; Berry, N. G.; Purton, J. A.; Adams, D. J.; Rosseinsky, M. J.,
30 452 Guest-adaptable and water-stable peptide-based porous materials by imidazolate side chain control.
31 453 *Angew. Chem. Int. Ed. Engl.* **2014**, 53, (1), 193-8.
32 454 (14) Thomas-Gipson, J.; Pérez-Aguirre, R.; Beobide, G.; Castillo, O.; Luque, A.; Pérez-Yáñez, S.; Román,
33 455 P., Unravelling the Growth of Supramolecular Metal-Organic Frameworks Based on Metal-Nucleobase
34 456 Entities. *Crystal Growth & Design* **2015**, 15, (2), 975-983.
35 457 (15) Hintz, H.; Wuttke, S., Postsynthetic modification of an amino-tagged MOF using peptide coupling
36 458 reagents: a comparative study. *Chem. Commun. (Camb.)* **2014**, 50, (78), 11472-5.
37 459 (16) Bonnefoy, J.; Legrand, A.; Quadrelli, E. A.; Canivet, J.; Farrusseng, D., Enantiopure
38 460 Peptide-Functionalized Metal-Organic Frameworks. *J. Am. Chem. Soc.* **2015**, 137, (29), 9409-16.
39 461 (17) Smaldone, R. A.; Forgan, R. S.; Furukawa, H.; Gassensmith, J. J.; Slawin, A. M.; Yaghi, O. M.;
40 462 Stoddart, J. F., Metal-organic frameworks from edible natural products. *Angew. Chem. Int. Ed. Engl.*
41 463 **2010**, 49, (46), 8630-4.
42 464 (18) Wei, Y.; Han, S.; Walker, D. A.; Fuller, P. E.; Grzybowski, B. A., Nanoparticle core/shell architectures
43 465 within MOF crystals synthesized by reaction diffusion. *Angew. Chem. Int. Ed. Engl.* **2012**, 51, (30),
44 466 7435-9.
45 467 (19) Furukawa, Y.; Ishiwata, T.; Sugikawa, K.; Kokado, K.; Sada, K., Nano- and Microsized Cubic Gel
46 468 Particles from Cyclodextrin Metal-Organic Frameworks †. *Angew. Chem. Int. Ed.* **2012**, 51, (42),

- 1
2
3 469 10566–10569.
4 470 (20) Botao Liu, H. L., Xiaonan Xu, Xue Li, Nana Lv, Vikramjeet Singh, J. Fraser Stoddart, Peter York, Xu
5 471 Xu, Ruxandra Gref, Jiwen Zhang, Optimized synthesis and crystalline stability of γ -cyclodextrin
6 472 metal-organic frameworks for drug adsorption. *Int. J. Pharm.* **2016**.
7
8 473 (21) Forgan, R. S.; Smaldone, R. A.; Gassensmith, J. J.; Furukawa, H.; Cordes, D. B.; Li, Q.; Wilmer, C. E.;
9 474 Botros, Y. Y.; Snurr, R. Q.; Slawin, A. M.; Stoddart, J. F., Nanoporous carbohydrate metal-organic
10 475 frameworks. *J. Am. Chem. Soc.* **2012**, 134, (1), 406-17.
11 476 (22) Trott, O.; Olson, A. J., AutoDock Vina: Improving the speed and accuracy of docking with a new
12 477 scoring function, efficient optimization, and multithreading. *J. Comput. Chem.* **2010**, 31, (2), 455–461.
13 478 (23) Choi, J.-S.; Son, W.-J.; Kim, J.; Ahn, W.-S., Metal-organic framework MOF-5 prepared by
14 479 microwave heating: Factors to be considered. *Microporous Mesoporous Mater.* **2008**, 116, (1-3),
15 480 727-731.
16 481 (24) Umemura, A.; Diring, S.; Furukawa, S.; Uehara, H.; Tsuruoka, T.; Kitagawa, S., Morphology design
17 482 of porous coordination polymer crystals by coordination modulation. *J. Am. Chem. Soc.* **2011**, 133,
18 483 (39), 15506-13.
19 484 (25) Brar, T.; Paul France, A.; Smirniotis, P. G., Control of Crystal Size and Distribution of Zeolite A. *Ind.*
20 485 *Eng. Chem. Res.* **2001**, 40, (4).
21 486 (26) Lethbridge, Z. A. D.; Williams, J. J.; Walton, R. I.; Evans, K. E.; Smith, C. W., Methods for the
22 487 synthesis of large crystals of silicate zeolites. *Microporous Mesoporous Mater.* **2005**, 79, (1-3),
23 488 339-352.
24 489 (27) Jhung, S. H.; Ji, H. L.; Chang, J. S., Crystal size control of transition metal ion-incorporated
25 490 aluminophosphate molecular sieves: Effect of ramping rate in the syntheses. *Microporous &*
26 491 *Mesoporous Materials* **2008**, 112, (1–3), 178-186.
27 492 (28) Lv, N.; Guo, T.; Liu, B.; Wang, C.; Singh, V.; Xu, X.; Li, X.; Chen, D.; Gref, R.; Zhang, J., Improvement
28 493 in Thermal Stability of Sucralose by gamma-Cyclodextrin Metal-Organic Frameworks. *Pharm. Res.*
29 494 **2016**.
30 495 (29) Chen, M.; Wang, Z.; Han, D.; Gu, F.; Guo, G., High-sensitivity NO₂ gas sensors based on flower-like
31 496 and tube-like ZnO nanomaterials. *Sensors Actuators B: Chem.* **2011**, 157, (2), 565-574.
32 497 (30) Qiu, M.; Chen, C.; Li, W., Rapid controllable synthesis of Al-MIL-96 and its adsorption of
33 498 nitrogenous VOCs. *Catal. Today* **2015**, 258, 132-138.
34 499 (31) Crini, G.; Peindy, H., Adsorption of C.I. Basic Blue 9 on cyclodextrin-based material containing
35 500 carboxylic groups. *Dyes and Pigments* **2006**, 70, (3), 204-211.
36
37
38
39
40
41
42
43
44 501
45
46
47
48
49
50
51
52
53
54
55
56
57
58
59
60

502 **For Table of Contents Use Only**

503 **Manuscript title:**

504 Microwave-assisted rapid synthesis of γ -cyclodextrin metal-organic frameworks for
505 size control and efficient drug loading

506 **Author list:**

507 Botao Liu^{1,2,a}, Yaping He^{1,3,a}, Liping Han¹, Vikramjeet Singh¹, Xiaonan Xu¹, Tao
508 Guo¹, Fanyue Meng¹, Xu Xu², Peter York¹, Zhaoxin Liu^{2,*}, Jiwen Zhang^{1,2,3,*}

509 **Affiliations:**

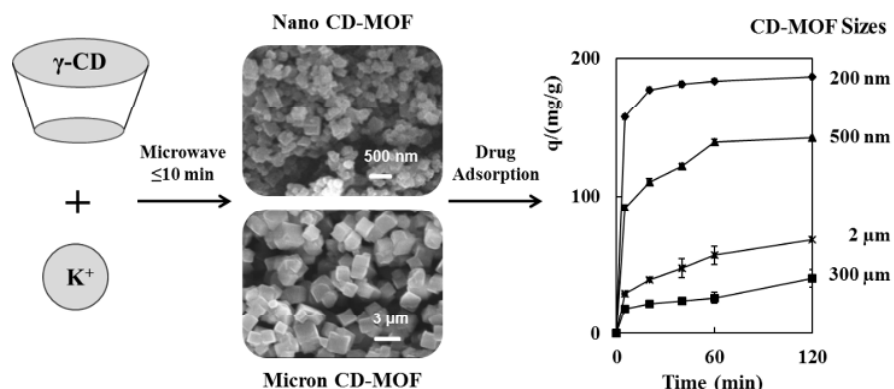
510 ¹ Center for Drug Delivery Systems, Shanghai Institute of Materia Medica, Chinese Academy of
511 Sciences, Shanghai 201210, China

512 ² School of Chemical and Environmental Engineering, Shanghai Institute of Technology, Shanghai
513 201418, China

514 ³ University of Chinese Academy of Sciences, Beijing 100049, China

515 ^a: Who contributed equally to the manuscript

516 **TOC graphic:**



517

518 **Synopsis:**

519 γ -CD-MOFs were synthesized by microwave-assisted technique for the first time and
520 exploited for drug delivery applications. The size and morphology of γ -CD-MOF
521 crystals can be efficiently controlled by optimizing the synthesis process. Compared
522 with micron crystals, nanometer sized γ -CD-MOFs (100-300 nm) showed rapid and
523 higher adsorption ($196 \text{ mg} \cdot \text{g}^{-1}$) of Fenbufen which implies the good loading
524 characteristics of γ -CD-MOFs.

525